NREL/TP-442-6912 • UC Category 1211 • DE95009264

CONF-950116--8

Dynamic Stall Occurrence on a Horizontal Axis Wind Turbine Blade

Derek E. Shipley
Mark S. Miller
Michael C. Robinson
University of Colorado
Boulder, Colorado

Prepared for
Fourteenth ASME-ETCE
Wind Energy Symposium
January 29-February 1, 1995
Houston, Texas

National Renewable Energy Laboratory
1617 Cole Boulevard
Golden, Colorado 80401-3393
A national laboratory of the U.S. Department of Energy
Managed by Midwest Research Institute
for the U.S. Department of Energy
under contract No. DE-AC36-83CH10093

Prepared under Task No. WE518110

July 1995

DISTRIBUTION OF THIS DOCUMENT IS UNLIMITED

NOTICE

This report was prepared as an account of work sponsored by an agency of the United States government. Neither the United States government nor any agency thereof, nor any of their employees, makes any warranty, express or implied, or assumes any legal liability or responsibility for the accuracy, completeness, or usefulness of any information, apparatus, product, or process disclosed, or represents that its use would not infringe privately owned rights. Reference herein to any specific commercial product, process, or service by trade name, trademark, manufacturer, or otherwise does not necessarily constitute or imply its endorsement, recommendation, or favoring by the United States government or any agency thereof. The views and opinions of authors expressed herein do not necessarily state or reflect those of the United States government or any agency thereof.

Available to DOE and DOE contractors from:
Office of Scientific and Technical Information (OSTI)
P.O. Box 62
Oak Ridge, TN 37831
Prices available by calling (615) 576-8401

Available to the public from:
National Technical Information Service (NTIS)
U.S. Department of Commerce
5285 Port Royal Road
Springfield, VA 22161
(703) 487-4650

Printed on paper containing at least 50% wastepaper and 10% postconsumer waste

DISCLAIMER

Portions of this document may be illegible in electronic image products. Images are produced from the best available original document.

DYNAMIC STALL OCCURRENCE ON A HORIZONTAL AXIS WIND TURBINE BLADE

D.E. SHIPLEY, M.S. MILLER, AND M.C. ROBINSON
DEPARTMENT OF AEROSPACE ENGINEERING SCIENCES
UNIVERSITY OF COLORADO
BOULDER, COLORADO

ABSTRACT

Surface pressure data from the National Renewable Energy Laboratory's "Combined Experiment" were analyzed to provide a statistical representation of dynamic stall occurrence on a downwind horizontal axis wind turbine (HAWT). Over twenty thousand blade rotational cycles were each characterized at four span locations by the maximum leading edge suction pressure and by the azimuth, velocity, and yaw at which it occurred. Peak suction values at least twice that seen in static wind tunnel tests were taken to be indicative of dynamic stall. The occurrence of dynamic stall at all but the inboard station (30% span) shows good quantitative agreement with the theoretical limits on inflow velocity and yaw that should yield dynamic stall. Two hypotheses were developed to explain the discrepancy at 30% span. Estimates are also given for the frequency of dynamic stall occurrence on upwind turbines. Operational regimes were identified which minimize the occurrence of dynamic stall events.

INTRODUCTION

The lifetime of major wind turbine components is typically far less than their 20-30 year design lifetime (Lynette, 1989). Components, such as generators and blades, are frequently subjected to dynamic loading far in excess of their design loads. A primary source of the excessive fatigue and failure is speculated to be derived from the unsteady aerodynamic operating environment experienced by turbines in the field. Unsteady aerodynamic effects, including dynamic inflow, turbulence, and dynamic stall, provide the driving mechanism for structural failure.

Previous investigations by these authors have illustrated the structural implications of one of these effects, dynamic stall (Shipley et al., 1994). This study showed the increase in aerodynamic loads that occurred from dynamic stall and the attendant large increases in structural forces and bending moments. Other research efforts have shown that dynamic stall can be driven by abrupt changes in inflow velocity, operation at yaw, blade passage through the tower shadow, turbulence, and wind shear (Butterfield, 1989; Robinson et al., 1994; Madsen, 1991).

Although the occurrence of horizontal axis wind turbine (HAWT) dynamic stall has been well documented and its effects are known, it is not clear if the frequency of occurrence warrants concern. This study provides a statistical examination of the occurrence of dynamic stall on horizontal axis wind turbine blades and documents the inflow conditions at which a turbine blade (or blade section) is most likely to experience the phenomena. The current project represents a first attempt to quantify the frequency of dynamic stall occurrence on a HAWT blade under a wide variety of field operating inflow conditions.

EXPERIMENTAL TEST SETUP

NREL's Combined Experiment horizontal axis wind turbine (Figure 1) is a 10.1 meter diameter, three-bladed downwind machine that rotates at a constant 72 RPM and is capable of producing 20 kW of power. The turbine is supported on a 0.4 meter diameter cylindrical tower at a height of 17 meters from the ground to the center of the hub. The blades are rectangular, untwisted NREL S809 airfoil sections with a 0.457 meter chord. One of the three blades was thoroughly instrumented with pressure transducers (Figure 2) at four different span locations (30%, 47%, 63%, and 80% span). Dynamic pressure and angle of attack were also measured at or near these four span locations. The data sample rate (521 Hz) was sufficient to capture the dynamic and transient pressure events elicited from time variant inlet flow conditions. The inlet flow magnitude and direction

MASTER

DISTRIBUTION OF THIS DOCUMENT IS UNLIMITED

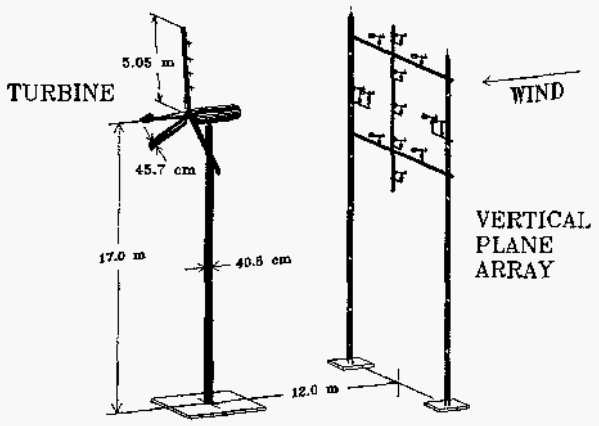

FIGURE 1: VIEW OF THE COMBINED EXPERIMENT TEST SITE INCLUDING THE GRUMMAN WIND STREAM 33 HORIZONTAL AXIS WIND TURBINE AND THE VERTICAL PLANE ARRAY.

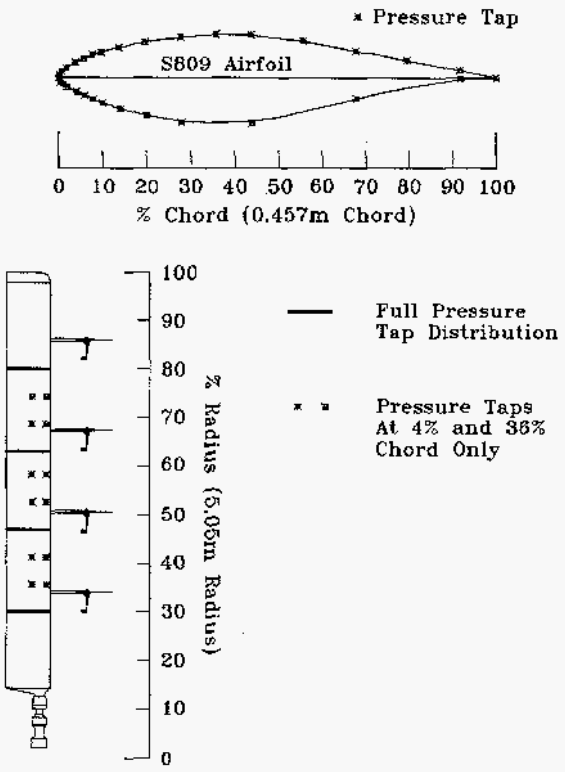

FIGURE 2: ROTOR BLADE CROSS SECTION AND LONGITUDINAL VIEWS SHOWING CHORDWISE PRESSURE TAP DISTRIBUTION AT FOUR PRIMARY LOCATIONS (30%, 47%, 63%, AND 80% SPAN).

were measured by the Vertical Plane Array located 12 meters upwind of the turbine. For a complete description of the Combined Experiment test setup and instrumentation see Butterfield et al. (1992).

TABLE 1: A PORTION OF THE DATABASE USED TO IDENTIFY DYNAMIC STALL EVENTS WITHIN INDIVIDUAL ROTATIONAL CYCLES.

Tape	Cyc	Span	Vel (m/s)	Yaw (deg)	Peak Cp	Az (deg)
d066012	2	30	11.184	5.56	-9.0389	196.5191
d066012	2	47	11.133	6.147	-7.4166	227.098
d066012	2	63	11.132	6.948	-7.1008	313.0493
d066012	2	80	11.132	6.948	-3.3914	316.3551
d066012	3	30	10.887	-0.418	-11.6249	187.8338
d066012	3	47	10.887	-0.418	-10.8553	212.0595
d066012	3	63	10.733	2.538	-6.8415	279.7242
d066012	3	80	10.733	2.538	-3.0639	284.7364

Data was collected over a wide range of inflow conditions representing the nominal operating environment of the turbine. A total of 59 five-minute episodes representing 20,577 complete rotational cycles of the instrumented blade were recorded to optical disk.

DYNAMIC STALL OCCURRENCE

A dynamic stall event occurs on a blade section when the local angle of attack rapidly increases through the static stall point. Turbulence, shifts in wind direction or magnitude, wind shear, or upstream flow disturbances can alter the local velocity, and hence, create blade angle of attack changes sufficient to drive dynamic stall.

Dynamic stall can be characterized by an extremely large suction peak value at or near the leading edge. Therefore, a database was created that characterized all four span locations for every rotational cycle of data by the maximum leading edge suction coefficient. The database also included the instantaneous inflow velocity, yaw, and azimuth angle at which the suction maximum occurred, and the tape name, cycle number, and span location. A portion of this database is shown in Table 1.

For this study, dynamic stall was assumed to occur if the peak pressure coefficient (C_p) was less than -10. This value is twice the maximum suction seen in wind tunnel tests of the S809 airfoil at Colorado State University (Butterfield et al., 1992). The use of such a low C_p value precludes the inclusion of some dynamic stall events. Therefore, the numbers presented in this report represent conservative estimates of the frequency of dynamic stall occurrence.

The maximum suction database was initially utilized to examine the frequency of dynamic stall occurrence across all 20,577 rotational cycles in the Combined Experiment data set. Figure 3 shows the percentage of all cycles in which dynamic stall occurred at any azimuthal angle. In addition, the frequency of dynamic stall occurrence at azimuthal angles not within the tower shadow region is shown for comparison. The tower shadow region was defined to be the azimuthal angles from 150° - 240°. The region was not centered at 180° (directly behind the

tower) because the increase in angle of attack necessary to drive dynamic stall occurs as the blade emerges from the tower shadow.

Removing the effects of the tower shadow gives an indication of the frequency of dynamic stall occurrence on upwind turbines. These values are somewhat conservative since dynamic stall could occur on an upwind turbine within the 150° - 240° azimuthal region. These events are driven by large changes in angle of attack induced by operation at high positive yaw angles.

From Figure 3, over 14% of all cycles exhibit dynamic stall at some point in the cycle at 30% span. This number drops significantly to only 2% at 80% span. This data suggests that upwind turbines might experience dynamic stall only 1% - 2% of the time. These statistics, however, may be misleading.

Figure 4 illustrates the distribution of inflow conditions over the entire Combined Experiment test. Each cycle was binned on inflow velocity and yaw, with the contours representing the total number of cycles corresponding to those inflow conditions. Clearly, the data is skewed towards low inflow velocities and 0° yaw. Since an untwisted blade was used on this phase of the Combined Experiment, at any given inflow velocity the angle of attack is highest inboard and lowest at the outboard station. The inflow velocity during a majority of the cycles was not sufficient to cause angles of attack that would put the 80% blade section into a stalled condition. Hence, a vast majority of the time dynamic stall could not have occurred at 80% span. This biases the existing data set and suggests an approach based on the frequency of dynamic stall occurrence under specific sets of inflow conditions.

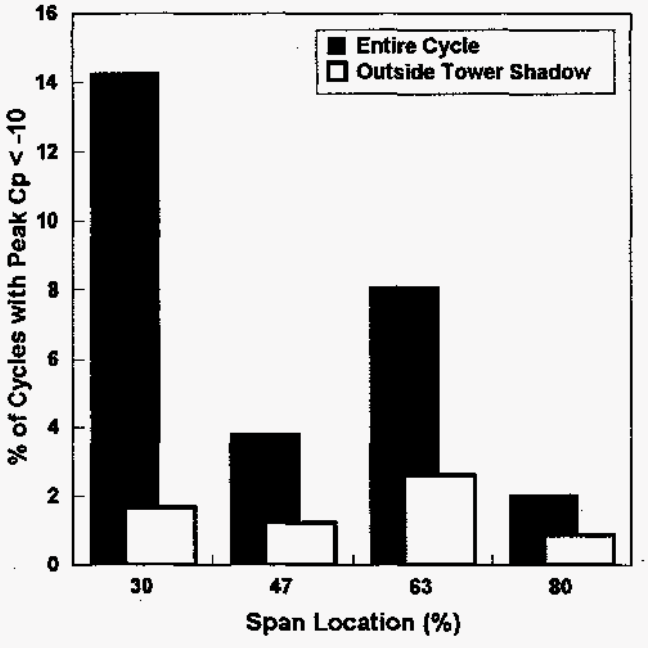

FIGURE 3: FREQUENCY OF DYNAMIC STALL OCCURRENCE OVER THE ENTIRE COMBINED EXPERIMENT DATA SET. AN INDICATION OF THE FREQUENCY OF DYNAMIC STALL OCCURRENCE ON UPWIND HAWTS IS GIVEN BY THE ELIMINATION OF THE TOWER SHADOW EFFECT.

DYNAMIC STALL OCCURRENCE UNDER VARIOUS INFLOW CONDITIONS

To gain some insight into the frequency of dynamic stall occurrence under various inflow conditions, the criteria established to identify dynamic stall ($C_p < -10$) was applied to the data of Figure 4 at all four span locations. The results are plotted in Figure 5 with the contours representing the percentage of cycles with the given inflow conditions that have a minimum leading edge $C_p < -10$, indicating a dynamic stall event.

To ascertain if these large magnitude pressure events are actually dynamic stall, a theoretical region was calculated in which dynamic stall is expected to occur. For a dynamic stall event to be initiated, the blade section angle of attack must rapidly increase through the static stall angle (~ 18° for this airfoil). A region was therefore calculated, using the methods of Shipley et al. (1995) for each blade station, in which the local angle of attack would pass through the stall angle during some portion of the cycle. The angle of attack model is based on inflow geometry relative to the turbine and models the tower shadow as a cosine function with a maximum velocity deficit of 30% of freestream.

The lower and upper limits of this region were overlaid as dashed lines on the data in Figure 5 and divide each plot into three regions. In the left region the modeled local angle of attack never exceeds 18°, and the blade should never be stalled. The region on the right corresponds to inflow conditions under which the modeled local angle of attack never decreases below 18°, and the blade should remain stalled throughout the cycle. The center region between the never-stalled and always-stalled limits is the regime in which dynamic stall is likely to exist.

Clearly, there is good quantitative agreement between the experimental data and the theoretical limits on dynamic stall occurrence at the outboard three span locations (47%, 63%, and 80% span). This indicates that the majority of large magnitude suction events (minimum $C_p < -10$) are due to the occurrence of

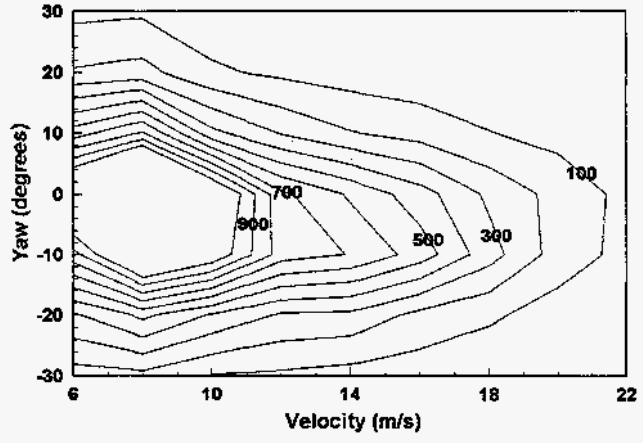

FIGURE 4: THE DISTRIBUTION OF INFLOW CONDITIONS OVER ALL 20,577 BLADE ROTATIONAL CYCLES IN THE COMBINED EXPERIMENT DATA SET. THE CONTOURS REPRESENT THE TOTAL NUMBER OF CYCLES CORRESPONDING TO EACH SET OF INFLOW CONDITIONS. THE DATA SET IS SKEWED TOWARDS LOWER VELOCITIES AND 0° YAW.

dynamic stall driven by changes in angle of attack from operation at yaw angles other than 0° or blade passage through the tower shadow.

There is an extremely high frequency of dynamic stall occurrence at both high positive and negative yaw angles and an apparent minimum in dynamic stall occurrence at approximately -10°. For instance, at 63% span, a velocity of 18 m/s, and a yaw of 10°, a dynamic stall event can be expected over 50% of the time. At this set of inflow conditions dynamic stall occurs over six times more frequently than for the data set as a whole.

To obtain an estimate of the frequency of dynamic stall occurrence on upwind turbines, the data of Figure 5 was further limited to include only those cases in which the leading edge suction peak occurred at azimuth angles outside of the tower shadow region (150° - 240° azimuth). Figure 6 shows that for this case, dynamic stall predominantly occurs at higher yaws (> ± 15°). With the tower shadow effect removed, these instances of dynamic stall are driven by changes in angle of attack resulting from wind shear, turbulence, or yawed flow. In fact, at the 63% span location a minimum $C_p < -10$ is found in more than 40% of the cycles at inflow velocities near 16 m/s under highly yawed conditions. Since upwind turbines often operate at yaws of 30° - 40°, it is clear that dynamic stall could be a significant problem.

Unlike the outer three span locations, the occurrence of high magnitude suction events at 30% span is not bracketed by the theoretical limits on dynamic stall occurrence (Figure 5 and 6). Either these events are not due to dynamic stall or the model does not predict dynamic stall occurrence under the proper conditions. The shape of the data distribution is very similar to the shape of the theoretical region of dynamic stall occurrence, suggesting that the second of these possibilities is most likely. It appears that at 30% span, dynamic stall occurs at higher inflow velocities than would be predicted from the theoretical model.

Working under this assumption, two hypotheses have been developed to explain this phenomena. First, three-

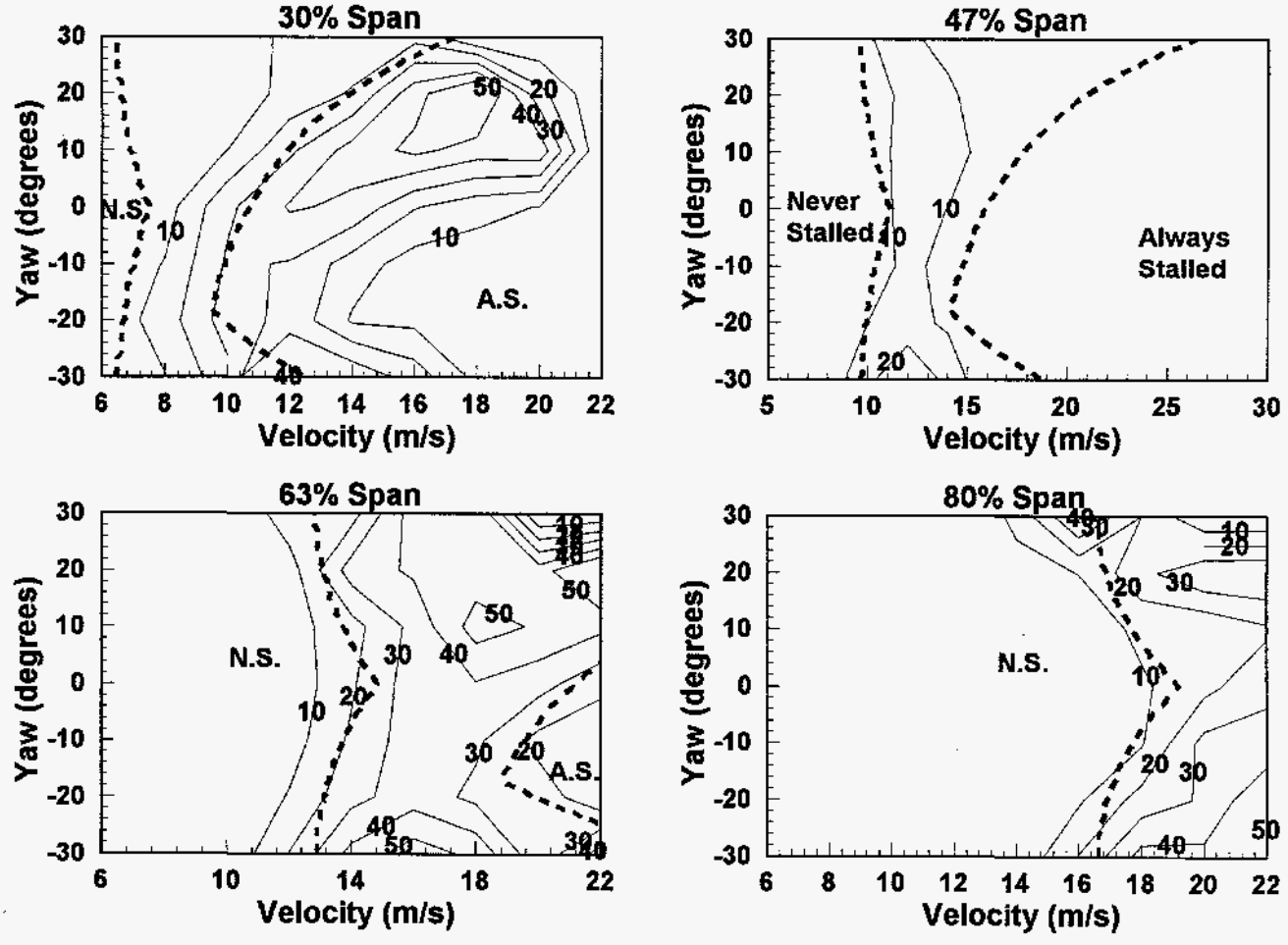

FIGURE 5: THE FREQUENCY OF DYNAMIC STALL OCCURRENCE OVER THE ENTIRE NORMAL OPERATING ENVIRONMENT OF THE COMBINED EXPERIMENT TURBINE. THE DASHED LINES BRACKET THE REGION IN WHICH DYNAMIC STALL COULD THEORETICALLY OCCUR.

dimensionality near the blade root might cause a delay in stall onset. Second, a larger tower shadow deficit at 30% span than at outboard stations would cause the angle of attack to decrease below 18° during a cycle at much higher inflow velocities than predicted by the angle of attack model. A combination of the two effects is also possible.

Evidence for the first hypothesis can be seen in pressure distributions at 30% span under conditions in which the blade section should be in deep stall. Figure 7 compares a typical 30% span pressure distribution to one measured in the CSU wind tunnel. Both distributions are for an angle of attack of approximately 30°. It is clear that the flow environment at the inboard station must deviate substantially from the steady, two-dimensional flow of the wind tunnel. This does not appear to be a machine-dependent phenomenon since similar effects have been reported by researchers examining other machines (Ronsten, 1992; Barnsley and Wellicome, 1992).

Research on the effect of rotation on flow separation has not been extensive; however, the results of Banks and Gadd (1963) showed that rotation has the effect of postponing separation, particularly at inboard stations. Narramore and Vermeland (1992) used a Navier-Stokes code to confirm these results and showed that flow three-dimensionality allowed the flow to remain attached at angles at which blade/momentum theory predicts massive separation.

It is also possible that a three-dimensional flow environment could be created near the root of the blade due to flow blockage upwind of the rotor. However, since upwind turbines also seem to experience an inboard stall delay, that possibility is less likely.

The second hypothesis is that the tower shadow deficit is larger at 30% span than at outboard stations. This would have the effect of shifting the region in which dynamic stall is theoretically likely to occur to higher velocities. To ascertain the

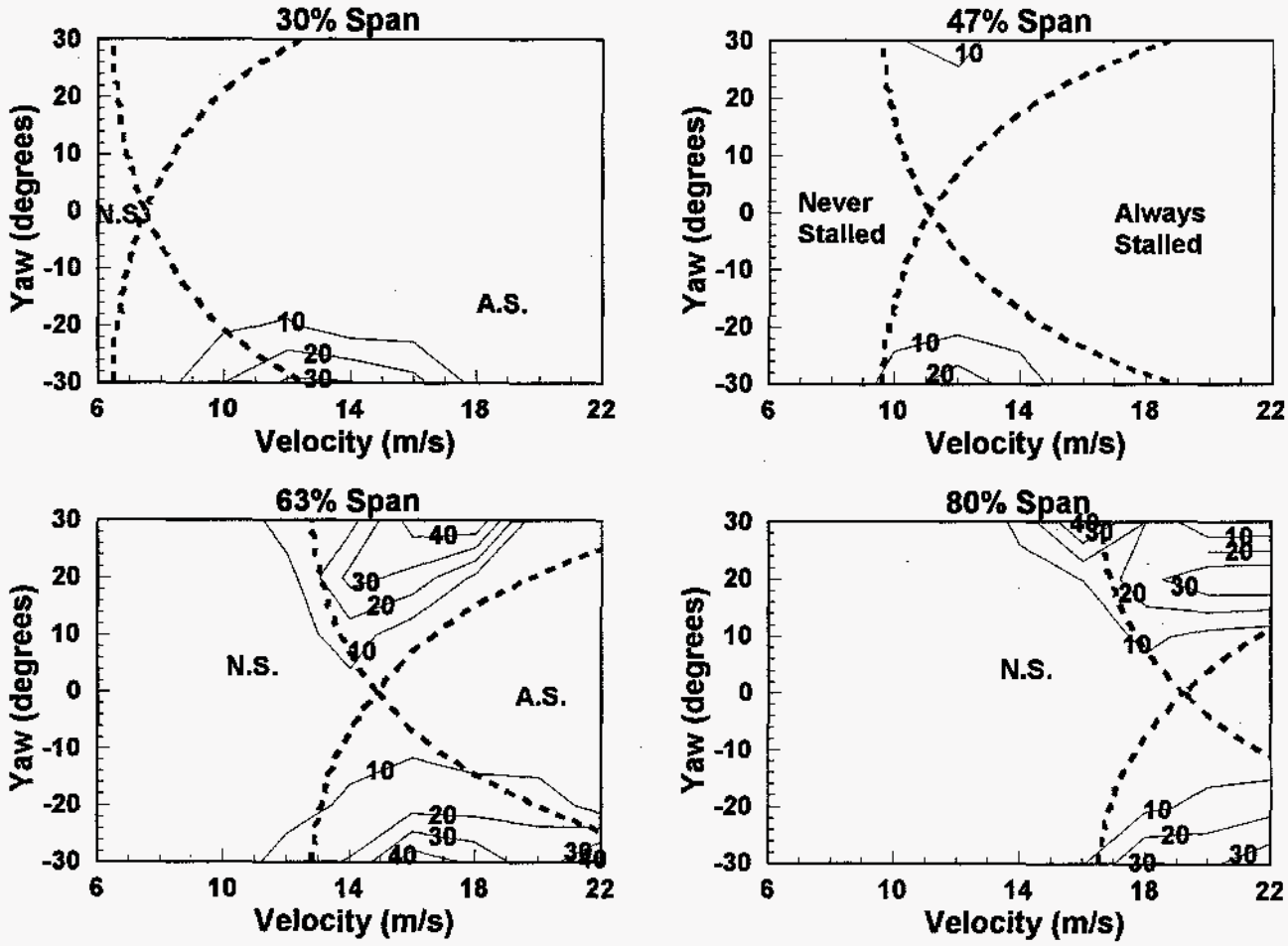

FIGURE 6: THE FREQUENCY OF DYNAMIC STALL OCCURRENCE AT AZIMUTHAL ANGLES OUTSIDE THE TOWER SHADOW REGION. THE DASHED LINES BRACKET THE REGION IN WHICH DYNAMIC STALL COULD THEORETICALLY OCCUR.

validity of this theory, a study based on measured angle of attack was performed. Measured angle of attack from 70 rotational cycles at 0° yaw was examined, and the minimum (within the tower shadow) and the mean (outside the tower shadow) angles of attack were identified. The respective inflow velocities were then calculated from these values and an estimate of the tower shadow deficit was made. The results for 30% and 63% span are shown in Figure 8. The mean tower deficit at 30% span is approximately 40%, compared to 25% at 63% span. The distribution at 30% span also displays far more variability. These effects may be caused by increased turbulence levels due to interaction between flow around the nacelle and the tower.

MINIMIZING THE OCCURRENCE OF DYNAMIC STALL

One strategy that could be used to minimize the damaging effects of dynamic stall is to operate the turbine under conditions which do not give rise to the phenomena. Since turbine operators have some nominal measure of control over turbine yaw, and none on wind velocity, a range of yaws is sought that would minimize dynamic stall occurrence across the entire velocity spectrum. From Figure 5, an operational regime between -20° - 0° yaw corresponds to an inflow velocity range where dynamic stall occurrence is at a minimum for this particular blade.

Of course, it is likely that the largest structural forces arise when dynamic stall occurs over large portions of the blade at or about the same time. Therefore, to model this potential event, the frequency of dynamic stall occurrence at two or more span locations during the same cycle was plotted in Figure 9. Although the frequency of dynamic stall occurrence is not as high, similar trends are noted. A strong peak in dynamic stall occurrence (> 40%) occurs for high positive yaw, and the frequency of dynamic stall occurrence is at a minimum at approximately -10° yaw. This data strengthens the observation that operation at moderately negative yaw angles minimizes the occurrence of dynamic stall.

This conclusion violates the normal operational paradigm that a turbine should be run at 0° yaw. However, Shipley et al. (1994) found that operation at modest yaw angles (± 20°) has no effect on the mean electrical power output. Therefore, for this turbine a setpoint of -10° yaw (rather than 0°) would minimize damaging dynamic loads while maintaining the same level of power output.

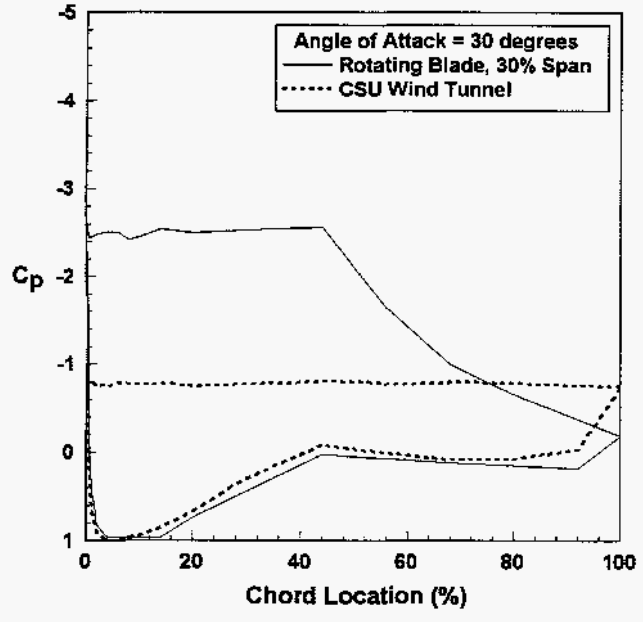

FIGURE 7: A COMPARISON BETWEEN A PRESSURE DISTRIBUTION MEASURED AT 30% SPAN AND ONE MEASURED IN THE CSU WIND TUNNEL. THE LOCAL ANGLE OF ATTACK OF 30° INDICATES THAT THE BLADE SHOULD BE IN DEEP STALL.

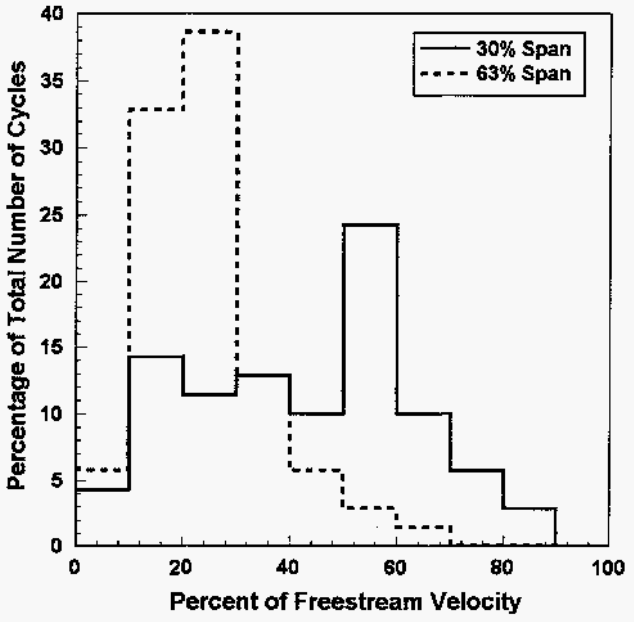

FIGURE 8: A HISTOGRAM OF THE MAXIMUM TOWER SHADOW DEFICIT AT 30% AND 63% SPAN. THE MEAN DEFICIT MAGNITUDE AT THE INBOARD STATION (30%) IS 15% GREATER THAN AT OUTBOARD STATIONS.

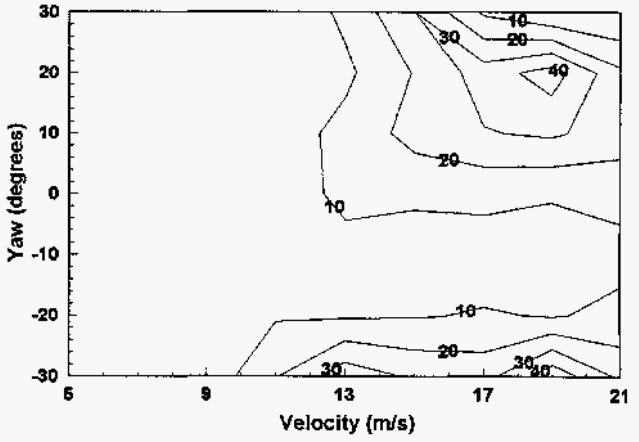

FIGURE 9: THE FREQUENCY OF DYNAMIC STALL OCCURRENCE AT TWO OR MORE SPAN LOCATIONS DURING THE SAME CYCLE.

CONCLUSION

The Combined Experiment data set was analyzed to provide a quantitative assessment of the frequency of dynamic stall occurrence on a downwind HAWT over the full range of normal operating conditions. Inflow regimes were identified that give rise to substantial occurrence of dynamic stall. Under the proper combination of inflow conditions, dynamic stall was evident in more than 50% of the recorded cycles. This figure is actually conservative since dynamic stall can occur with suction peaks of lower magnitudes.

Although this study was performed on a downwind turbine with untwisted blades, the results have significance for other downwind turbines, upwind turbines, and turbines with twisted and tapered blades. Operational regimes were defined based on inflow geometry relative to the turbine under which dynamic stall is likely to occur. Given the blade twist distribution and length, this region can easily be calculated using the technique of Shipley et al. (1995) for any blade. Thus, operational conditions that would give rise to a high incidence of dynamic stall can be identified.

Typical HAWT blades have a twist distribution such that the entire blade is at the same, or nearly the same, angle of attack for a given wind speed. Therefore, when dynamic stall occurs, it will affect extremely large portions of the blade at the same time. However, by adjusting blade pitch, the entire blade can be put into a operational regime in which dynamic stall is not likely to occur. Doing so should yield a significant reduction in rotor loads.

ACKNOWLEDGEMENTS

This work was sponsored in part by the U.S. Department of Energy under contract number DE-AC36-83CH10093.

REFERENCES

Banks, W.H.H., and Gadd, G.E., 1963, "Delaying Effect of Rotation on Laminar Separation", *AIAA Journal*, Vol. 1, pp. 941-942.

Barnsley, M.J., and Wellicome, J.F., 1992, "Wind Tunnel Investigation of Stall Aerodynamics for a 1.0 m Horizontal Axis Rotor", *Journal of Wind Engineering and Industrial Aerodynamics*, Vol. 39, pp. 11-21.

Butterfield, C.P., 1989, "Three-Dimensional Airfoil Performance Measurements on a Rotating Wind", *Proceedings of the European Wind Energy Conference*, Glasgow, Scotland.

Butterfield, C.P., Musial W.P., and Simms, D.A., 1992, "Combined Experiment Phase I Final Report", NREL/TP-257-4655, National Renewable Energy Laboratory, Golden, CO.

Lynette, R., 1989, "California Wind Farms: Operational Data Collection and Analysis", SERI/PR-217-3489, NREL, Golden, CO.

Madsen, H.A., 1991, "Aerodynamics of a Horizontal-Axis Wind Turbine in Natural Conditions", RISO-m-2903, Riso National Laboratory, Roskilde, Denmark.

Narramore, J.C., and Vermeland, R., 1992, "Navier-Stokes Calculations of Inboard Stall Delay Due to Rotation", *Journal of Aircraft*, Vol. 29, pp. 73-78.

Robinson, M.C., Luttges, M.W., Miller, M.S., Shipley, D.E., and Young, T.S., 1994, "Wind Turbine Blade Aerodynamics: The Analysis of Field Test Data", *13th ASME/ETCE Wind Energy Symposium Proceedings*, New Orleans, LA, pp. 9-16.

Ronsten, G., 1992, :Static Pressure Measurements on a Rotating and a Non-rotating 2.375 m Wind Turbine Blade. Comparison with 2D Calculations", *Journal of Wind Engineering and Industrial Aerodynamics*, Vol. 39, pp. 105-118.

Shipley, D.E., Miller, M.S., Robinson, M.C., Luttges, M.W., and Simms, D.A., 1994, "Evidence that Aerodynamic Effects, Including Dynamic Stall, Dictate HAWT Structural Loads and Power Generation in Highly Transient Time Frames", *AWEA Windpower 94 Proceedings*, Minneapolis, MN, pp. 615-626.

Shipley, D.E., Miller, M.S., Robinson, M.C., Luttges, M.W., and Simms, D.A., 1995, "Techniques for the Determination of Local Dynamic Pressure and Angle of Attack on a Horizontal Axis Wind Turbine", NREL/TP-442-7393, National Renewable Energy Laboratory, Golden, CO.